Sustainable Energy & Fuels

ROYAL SOCIETY OF CHEMISTRY

COMMUNICATION

View Article Online
View Journal | View Issue

Cite this: *Sustainable Energy Fuels*, 2022, **6**, 5072

Received 11th August 2022
Accepted 28th September 2022

DOI: 10.1039/d2se01105k

rsc.li/sustainable-energy

A stable platinum porphyrin based photocatalyst for hydrogen production under visible light in water†

Emmanouil Orfanos, [a] Kalliopi Ladomenou, *[b] Panagiotis A. Angaridis, [c] Theodoros Papadopoulos, [d] Georgios Charalambidis, [a] Maria Vasilopoulou [e] and Athanassios G. Coutsolelos *[af]

A stable system containing a Pt metalated porphyrin as a molecular solid photocatalyst in acidic aqueous solution is able to produce hydrogen efficiently, under visible light irradiation. The system shows a H_2 evolution rate of 467.3 μmol g^{-1} h^{-1}.

Solar hydrogen as a renewable energy solution is expected to be one of the leading options in the near future. This type of fuel could solve many environmental problems such as pollution and energy storage. Molecular hydrogen could start a revolution of "clean" energy as one of the most suitable solar fuels, providing high energy capacity and being environmentally friendly. Moreover, hydrogen fuel cells do not produce any CO_2 during operation, which eliminates environmental hazards. Hydrogen can be obtained in many ways such as electrolysis of water, petroleum cracking and photocatalytic hydrogen production from water. Among all the above the latter is simple, environmentally friendly and consumes less energy. Photocatalytic systems typically consist of a catalyst (C), a photosensitizer (PS) and a sacrificial electron donor (SED).[1] Porphyrins are a class of compounds that are used by nature in photosynthesis and other important biological reactions. Therefore, these molecules have been reported in the literature as photosensitizers in many hydrogen evolution systems.[2–4] Porphyrin dyes have strong light absorption in the visible region and are able to produce hydrogen in organic solvents or water,[5] and also in their mixtures.[6] As catalysts for hydrogen evolution, metal nanoparticles (mainly Pt) and metalated complexes, are commonly used.[3,7–10] Recently, many hydrogen evolving systems have been developed and comprised of just a photocatalyst (PC) and a SED.[11–17] These types of photocatalysts possess elaborated architectures that are quite difficult to prepare. Among these materials, porphyrin metal organic frameworks (MOFs) have been excessively used as photosensitizers for hydrogen evolution.[18–20] The main drawbacks of these systems are their poor stability in water and their complex synthetic procedures. In the literature there is only one example of a Pt porphyrin-based conjugated polyelectrolyte with quaternary ammonium salts in the side chains. This conjugate showed a significant photocatalytic H_2 evolution of 5.39 mmol g^{-1} h^{-1}. Moreover, there is an example of a platinum porphyrin photocatalyst with a pyridyl group anchored onto TiO_2 electrode.[21–23] This Pt metalated porphyrin is effective catalyst towards the photoelectrochemical hydrogen production from water. Since there are limited reports of a simple Pt porphyrin-based photocatalyst it is vital to synthesize and study such simple molecules as photocatalysts for H_2 evolution reaction. In most reports porphyrin molecules were mainly used a photosensitizers as a part of a metal organic framework or attached onto a semiconductor or assembled into a supramolecular architecture and Pt is photo deposited as catalyst.[4,7,24–26]

Herein we prepared a simple solid photocatalyst comprised of just a molecular platinum metalated porphyrin able to produce hydrogen in pure water in the presence of a sacrificial electron donor. Therefore, we synthesized three porphyrins **Pt-TEPP**, **Pt-TBPP** and **Pt-TPP** (Fig. 1) with different substituents at the *meso* position, possessing diverse electronic properties. These structural modifications can alter and optimize their energy bands, their absorption spectra and their packing arrangements in water. The presence of a Pt atom at the center of the porphyrin ring can improve the electronic structure and capability of the photocatalyst. The **Pt-TEPP** porphyrin proved to be more effective compared to the other two, since upon visible

[a]*University of Crete, Laboratory of Bioinorganic Chemistry, Voutes Campus, 70013, Heraklion, Crete, Greece. E-mail: acoutsol@uoc.gr*

[b]*International Hellenic University, Department of Chemistry, Laboratory of Inorganic Chemistry, Kavala Campus, Agios Loucas, 65404, Greece*

[c]*Aristotle University of Thessaloniki, Department of General and Inorganic Chemistry, Faculty of Chemistry, GR-54124 Thessaloniki, Greece*

[d]*Faculty of Science and Engineering, Thornton Science Park, University of Chester, CH2 4NU, Chester, UK*

[e]*Institute of Nanoscience and Nanotechnology, National Center for Scientific Research "Demokritos", 15341 Agia Paraskevi, Attica, Greece*

[f]*Institute of Electronic Structure and Laser (IESL) Foundation for Research and Technology – Hellas (FORTH), Vassilika Vouton, GR 70013 Heraklion, Crete, Greece*

† Electronic supplementary information (ESI) available. CCDC 2143453. For ESI and crystallographic data in CIF or other electronic format see https://doi.org/10.1039/d2se01105k

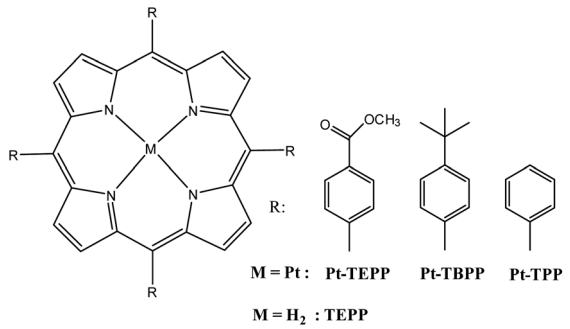

Fig. 1 Chemical structures of the photocatalysts.

light irradiation, was able to convert the protons of water into H_2. Moreover, in this study the experimental conditions were appropriate tuned in order to improve the H_2 production.

The preparation of all porphyrin derivatives were performed following already published procedures.[27] The final step involved the metalation of the porphyrin macrocycle with platinum, leading to the formation of the final products.[28] The mass (MALDI-TOF) and UV-Vis spectra of all the compounds are shown in Fig. S1–S4.† The molecular structure of **Pt-TEPP** was also determined by single crystal X-ray diffraction analysis (Tables S1–S3†). A view of its molecular structure is given in Fig. S5.† All bond distances and angles were found to be within the usual range for analogous *meso* substituted Pt(II) porphyrins (Tables S2 and S3†).

The concept of the present study is to use simple chromophores with immobilized platinum in the core of the porphyrin ring, as photocatalysts for H_2 evolution. Moreover, an alternative procedure that was studied herein is the photo deposition of platinum nanoparticles onto the free-base porphyrin dye.

In order to investigate the morphology and the elemental composition of **Pt-TEPP** photocatalyst, scanning electron microscopy (SEM) and energy dispersive spectroscopy (EDS) were utilized, respectively. The SEM images showed a uniform morphology of the photosensitizer (Fig. 2a), featuring a large surface area, which might benefit the photocatalytic hydrogen production of the system.[7,29–31] The EDS studies verified the elemental presence of the desired materials in the structure of the photocatalyst such as platinum, carbon, nitrogen and oxygen (Fig. S6†). In addition, SEM images for porphyrins **Pt-TBPP** and **Pt-TPP** were obtained (Fig. S7†). The morphology of both porphyrins was different compared to **Pt-TEPP**, featuring amorphous-like areas.

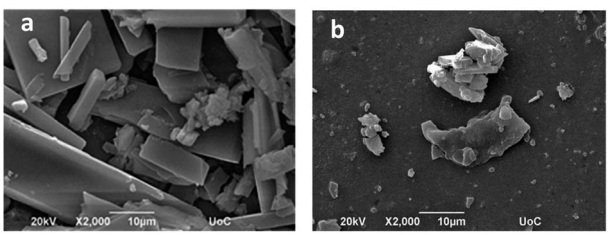

Fig. 2 SEM images of photocatalyst **Pt-TEPP** (a) before and (b) after the photocatalysis.

Table 1 Oxidation and reduction potentials of Pt-porphyrins *vs.* NHE[32]

Porphyrins	$E_{1/2}$ Ox (V)	$E_{1/2}$ Red (V)
Pt-TEPP	1.72	−0.91
Pt-TBPP	1.59	−1.08
Pt-TPP	1.62	−1.05

The absorption spectrum of **Pt-TEPP** was obtained in dichloromethane and in the solid state (Fig. S8†). The spectrum in solution is characteristic of a metalated Pt porphyrin, featuring an intense Soret band at 402 nm and two Q bands at 510 and 540 nm. The spectrum of the solid **Pt-TEPP** was slightly broadened and red shifted. The Soret band appeared at 428 nm and the Q-bands at 553 and 594 nm.

Cyclic voltammetry was contacted in order to compare the energy levels of the three photocatalysts and their redox potentials are shown in Table 1 (Fig. S9†). The ground state oxidation potentials ($E_{1/2}$ Ox) that correspond to the HOMO levels of the porphyrins **Pt-TEPP**, **Pt-TBPP** and **Pt-TPP** were calculated 1.72, 1.59 and 1.62 V, respectively. The measured reduction potentials ($E_{1/2}$ Red) that correspond to the LUMO levels are −0.91, −1.08 and −1.05 V for **Pt-TEPP**, **Pt-TBPP** and **Pt-TPP**, respectively. From the above measurements it can be concluded that the lower LUMO value of **Pt-TEPP** compared to the other two porphyrins, may increase the electron transfer rate from the photoexcited porphyrin to the central Pt atom/catalyst. This could enhance the photoinduced hydrogen production of the **Pt-TEPP** photocatalyst.

The molecular dipole moments of the three porphyrins were calculated using Density Functional Theory and were found $|\mu|$ = 0.674 D, 0.045 D and 0.027 D for **Pt-TEPP**, **Pt-TBPP** and **Pt-TPP**, respectively. The **Pt-TEPP** exhibits the largest dipole among the porphyrins, creating a difference in potential between the platinum and the terminal *meso* substituents (Fig. S10†). Therefore, the ester groups with the higher electronegativity result in larger molecular dipoles.

Subsequently, photocatalytic hydrogen production experiments were conducted; in order to asses the catalytic performance of each derivative. The platinum porphyrins were used as photocatalysts in aqueous solution in the presence of ascorbic acid (AA) 1 M as a sacrificial electron donor, at pH = 4.

Initially, we examined the influence of the quantity of the photocatalyst, towards the H_2 evolution activity. To this end different amounts (1 mg, 3 mg and 5 mg), of the **Pt-TEPP** photocatalyst were added in 5 mL of aqueous solution in the presence of 1 M AA. As shown in Fig. S11,† when 3 mg of **Pt-TEPP** was used the system proved to be more efficient producing almost three times more H_2 (2601 μmol g^{-1}) compared to 1 mg (750 μmol g^{-1}) and 5 mg (120 μmol g^{-1}). This can be attributed to better and more stable dispersion of the solid photocatalyst when 3 mg of **Pt-TEPP** were employed.

Interestingly, by altering the pH values of the aqueous solution at pH = 3 and pH = 5, no modification in the hydrogen production was observed. The amount of H_2 that was produced as a function of the reaction time is shown in Fig. 3. In order to

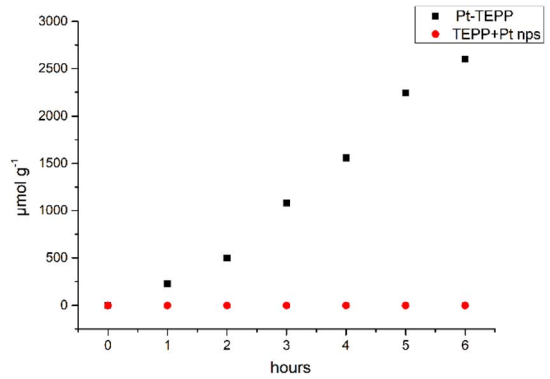

Fig. 3 Hydrogen evolution of Pt-TEPP and TEPP/Pt photocatalysts in aqueous solution of 1 M AA.

understand the need of platinum metalated porphyrin, the same free base porphyrin was used as a photosensitizer and Pt nanoparticles as catalysts. The added amount of Pt was the same as the Pt present in 3 mg of **Pt-TEPP**. Under the same experimental conditions, no H_2 was observed after 6 h of light irradiation (Fig. 3). The system was stirred for additional 24 hours in order to obtain well defined Pt nanostructures,[33] but still no H_2 was produced. Therefore, the presence of Pt in the porphyrin ring is essential for H_2 production in this type of system.

After 6 h of irradiation the rate of H_2 production was 467.3 μmol g^{-1} h^{-1} when 3 mg of **Pt-TEPP** photocatalyst was used in water at pH = 4.

The performance of our photocatalyst compared to recently reported porphyrin-based systems and the corresponding activities are listed in Table S4.† As shown in Table S4,† in some cases our system is more effective compared to other porphyrin based photocatalysts that work well only in the presence of Pt cocatalyst (entries 6 & 7). The photocatalytic stability of **Pt-TEPP** was investigated by repeating photocatalytic hydrogen production experiments. The system was irradiated for 6 h and then was kept in the dark overnight, then the sample was degassed and re-introduced for photocatalysis until the irradiation was re-started. As shown in Fig. 4, the production of hydrogen was

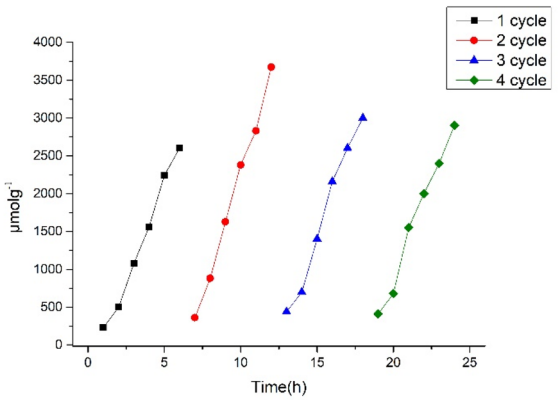

Fig. 4 Hydrogen evolution of Pt-TEPP photocatalyst in aqueous solution of 1 M AA.

slightly increased at the second cycle and at the next two cycles remained steady. This result clearly demonstrates that after light irradiation for four cycles (6 h per cycle) the **Pt-TEPP** photocatalyst remains stable.

In order to exclude the presence of Pt nanoparticles at the photocatalytic system, excess of mercury was added in the reaction mixture. After light irradiation under the same conditions, the photocatalytic system produced the same amount of H_2 as in the absence of mercury (Fig. S12†). Therefore, the Pt catalyst, situated inside the porphyrin ring is responsible for the H_2 evolution of this system.

Moreover, the catalytic performance of **Pt-TBPP** and **Pt-TPP** photocatalysts was also examined. In both Pt porphyrins no H_2 was detected after 6 hours of light irradiation under the same catalytic conditions. Only a small amount of H_2 was obtained after 23 h of irradiation (0.23 μmol for **Pt-TBPP** and 1.92 μmol for **Pt-TPP**). The remarkably enhanced H_2 evolution activity of **Pt-TEPP** compared to the other two porphyrins is mainly ascribed to three factors: (a) the higher exciton generation efficiency, (b) the greater induced dipole moment that promotes the photogeneration and transfer of electron/hole pairs, and (c) the better dispersibility of the molecule in the aqueous media.

In order to elucidate the state of the photocatalyst after the H_2 evolution experiments, UV-vis (Fig. S13†) and MALDI-TOF (Fig. S13†) spectra were recorded and showed that the **Pt-TEPP** remained intact after light irradiation. A SEM image was also obtained after the photocatalysis. As shown in Fig. 2b the morphology of **Pt-TEPP** was completely alerted, but the properties of the photocatalyst were retained. For that reason, **Pt-TEPP** can be recycled and used again in future photocatalytic experiments.

Moreover, the stability of **Pt-TEPP** during the photocatalysis for H_2 evolution was investigated by powder X-ray diffraction analysis. The powder X-ray diffraction pattern of the catalyst, as isolated from the crude reaction mixture after completion of the photocatalysis experiment, is depicted in Fig. S14.† Unfortunately, the low crystallinity of the sample resulted in relatively low-resolution X-ray diffraction data, and therefore indexing and space group determination were not possible to be performed. Nevertheless, a comparative analysis of the experimentally obtained data with the theoretically simulated powder X-ray diffraction patterns from the crystal structures of **TEPP**, **Pt-TEPP** and the **PtTEPP solid** that was used in our photocatalytic experiments (Fig. S15†), determined by single crystal X-ray diffraction analysis, appears to be very informative. Undoubtedly, the diffraction pattern of the solid (red color) is completely different from that of **TEPP** (green color), providing an indication that **Pt-TEPP** does not decompose to the free-base form and Pt(II) ions or Pt nanoparticles which could perform the catalytic conversion. In contrast, it seems that there is a good agreement in general positions and intensities of specific diffraction peaks with the simulated diffraction pattern of **Pt-TEPP** (blue color). For example, in the low-angle range the characteristic peaks at 2θ values of 5.9° and 7.7° can be assigned to the (100) and (002) sets of planes, respectively, as designated from the **Pt-TEPP** simulated pattern. The (200) peak observed at $2\theta = 11{,}8°$ is also common for the two compounds. Finally, the

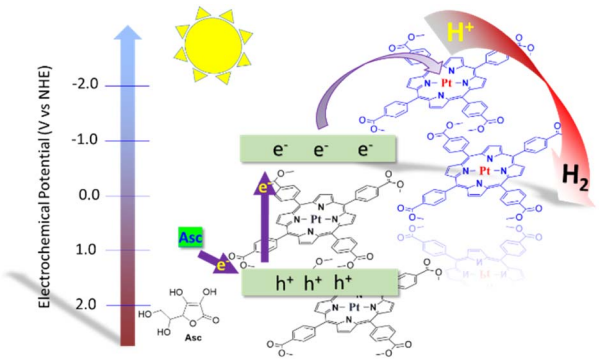

Fig. 5 Schematic diagram of the **Pt-TEPP** photocatalytic hydrogen evolution.

peaks observed at $2\theta = 13.6°$ and 19.8° can be assigned to (110) and (014), respectively. These features suggest a similarity of the structures of the two compounds. Small differences between the two diffraction patterns (slight shifts in the positions of specific diffraction peaks) in the middle- and high-angle region could be attributed to insignificant variations in the packing of the molecules in the isolated solid compared to the single-crystal molecular structure. Therefore, we can conclude that **Pt-TEPP** retains its structural integrity over the course of the photocatalytic H_2 production experiment.

The possible mechanism of hydrogen evolution reaction of **Pt-TEPP** photocatalyst is shown in Fig. 5. Since the photocatalyst is able to produce H_2 in the absence of a co-catalyst, the Pt atom at the center of the porphyrin ring can catalyze the proton reduction. The light is absorbed by the porphyrin molecule, the electrons are excited and then are transferred to the central Pt atoms generating hydrogen.[16,34]

In this report we presented a stable and a quite effective photocatalyst towards H_2 production in water. The system remained intact, even after 25 h of visible light irradiation. Since, the photocatalyst is not soluble in water, it can be recycled and re-used easily. When the porphyrin is metalated with Pt the system is able to produce H_2, with no further assistance of a co-catalyst. In contrast, when Pt nanoparticles are dispersed on the free-base porphyrin no H_2 production can be detected. The remarkably H_2 evolution activity of **Pt-TEPP** compared to **Pt-TBPP** and **Pt-TPP** was mainly due to its advanced exciton efficiency, to its effective generation and electron/hole pair transfer and its morphology in the aqueous phase. Moreover, this work demonstrates the use of a simple monomer molecule, as photocatalyst able to efficiently produce H_2 of 467.3 μmol g^{-1} h^{-1}, under visible light in water, in the absence of a cocatalyst.

Conflicts of interest

There are no conflicts to declare.

Acknowledgements

This research was funded by the General Secretariat for Research and Technology (GSRT) and Hellenic Foundation for Research and Innovation (HFRI; project code: 508). This research has also been co-financed by the European Union and Greek national funds through the Operational Program Competitiveness, Entrepreneurship, and Innovation, under the call RESEARCH–CREATE–INNOVATE (project code: T1EDK-01504). In addition, this research has been co-financed by the European Union and Greek national funds through the Regional Operational Program "Crete 2014-2020", project code OPS:5029187. Moreover, the European Commission's Seventh Framework Program (FP7/2007-2013) under grant agreement no. 229927 (FP7-REGPOT-2008-1, Project BIO-SOLENUTI) and the Special Research Account of the University of Crete are gratefully acknowledged for the financial support of this research.

Notes and references

1 T. S. Teets and D. G. Nocera, *Chem. Commun.*, 2011, **47**, 9268–9274.
2 H.-C. Chen, D. G. H. Hetterscheid, R. M. Williams, J. I. van der Vlugt, J. N. H. Reek and A. M. Brouwer, *Energy Environ. Sci.*, 2015, **8**, 975–982.
3 J. Kim, D. R. Whang and S. Y. Park, *ChemSusChem*, 2017, **10**, 1883–1886.
4 G. B. Bodedla, G. Tang, J. Zhao and X. Zhu, *Sustainable Energy Fuels*, 2020, **4**, 2675–2679.
5 A.-M. Manke, K. Geisel, A. Fetzer and P. Kurz, *Phys. Chem. Chem. Phys.*, 2014, **16**, 12029–12042.
6 T. Lazarides, M. Delor, I. V. Sazanovich, T. M. McCormick, I. Georgakaki, G. Charalambidis, J. A. Weinstein and A. G. Coutsolelos, *Chem. Commun.*, 2014, **50**, 521–523.
7 Y. Liu, L. Wang, H. Feng, X. Ren, J. Ji, F. Bai and H. Fan, *Nano Lett.*, 2019, **19**, 2614–2619.
8 Z. Zhang, Y. Zhu, X. Chen, H. Zhang and J. Wang, *Adv. Mater.*, 2019, **31**, 1806626.
9 V. Nikolaou, G. Charalambidis and A. G. Coutsolelos, *Chem. Commun.*, 2021, **57**, 4055–4058.
10 A. G. Coutsolelos, P. Angaridis, E. Orfanos and K. Ladomenou, *Dalton Trans.*, 2022, **51**, 8009–8014.
11 T. Banerjee, K. Gottschling, G. Savasci, C. Ochsenfeld and B. V. Lotsch, *ACS Energy Lett.*, 2018, **3**, 400–409.
12 L. Xie, J. Tian, Y. Ouyang, X. Guo, W. Zhang, U.-P. Apfel, W. Zhang and R. Cao, *Angew. Chem., Int. Ed.*, 2020, **59**, 15844–15848.
13 E. Nikoloudakis, M. Pigiaki, M. N. Polychronaki, A. Margaritopoulou, G. Charalambidis, E. Serpetzoglou, A. Mitraki, P. A. Loukakos and A. G. Coutsolelos, *ACS Sustainable Chem. Eng.*, 2021, **9**, 7781–7791.
14 M. Joseph and S. Haridas, *Int. J. Hydrogen Energy*, 2020, **45**, 11954–11975.
15 V. Nikolaou, G. Charalambidis, K. Ladomenou, E. Nikoloudakis, C. Drivas, I. Vamvasakis, S. Panagiotakis, G. Landrou, E. Agapaki, C. Stangel, C. Henkel, J. Joseph, G. Armatas, M. Vasilopoulou, S. Kennou, D. M. Guldi and A. G. Coutsolelos, *ChemSusChem*, 2021, **14**, 961–970.
16 X. Zhao, X. Zhang, Y. Liang, Z. Hu and F. Huang, *Macromolecules*, 2021, **54**, 4902–4909.

17 E. Nikoloudakis, I. López-Duarte, G. Charalambidis, K. Ladomenou, M. Ince and A. G. Coutsolelos, *Chem. Soc. Rev.*, 2022, **51**, 6965–7045.
18 C. Lin, C. Han, H. Zhang, L. Gong, Y. Gao, H. Wang, Y. Bian, R. Li and J. Jiang, *Inorg. Chem.*, 2021, **60**, 3988–3995.
19 H. Hu, Z. Wang, L. Cao, L. Zeng, C. Zhang, W. Lin and C. Wang, *Nat. Chem.*, 2021, **13**, 358–366.
20 Q. Zuo, T. Liu, C. Chen, Y. Ji, X. Gong, Y. Mai and Y. Zhou, *Angew. Chem., Int. Ed.*, 2019, **58**, 10198–10203.
21 K. Morita, K. Takijiri, K. Sakai and H. Ozawa, *Dalton Trans.*, 2017, **46**, 15181–15185.
22 K. Morita, K. Sakai and H. Ozawa, *ACS Appl. Energy Mater.*, 2019, **2**, 987–992.
23 K. Akamine, K. Morita, K. Sakai and H. Ozawa, *ACS Appl. Energy Mater.*, 2020, **3**, 4860–4866.
24 M. Zhu, Y. Dong, Y. Du, Z. Mou, J. Liu, P. Yang and X. Wang, *Chem. - Eur. J.*, 2012, **18**, 4367–4374.
25 J. Wang, Y. Zhong, L. Wang, N. Zhang, R. Cao, K. Bian, L. Alarid, R. E. Haddad, F. Bai and H. Fan, *Nano Lett.*, 2016, **16**, 6523–6528.
26 X. Yang, Z. Hu, Q. Yin, C. Shu, X.-F. Jiang, J. Zhang, X. Wang, J.-X. Jiang, F. Huang and Y. Cao, *Adv. Funct. Mater.*, 2019, **29**, 1808156.
27 L. R. Milgrom, R. J. Zuurbier, J. M. Gascoyne, D. Thompsett and B. C. Moore, *Polyhedron*, 1994, **13**, 209–214.
28 C. Stangel, D. Daphnomili, T. Lazarides, M. Drev, U. O. Krašovec and A. G. Coutsolelos, *Polyhedron*, 2013, **52**, 1016–1023.
29 A. M. Huerta-Flores, G. Bengasi, K. Baba and N. D. Boscher, *ACS Appl. Energy Mater.*, 2020, **3**, 9848–9855.
30 T.-F. Yeh, J.-M. Syu, C. Cheng, T.-H. Chang and H. Teng, *Adv. Funct. Mater.*, 2010, **20**, 2255–2262.
31 J. Yuan, J. Wen, Q. Gao, S. Chen, J. Li, X. Li and Y. Fang, *Dalton Trans.*, 2015, **44**, 1680–1689.
32 C. G. Zoski, *Handbook of Electrochemistry*, Elsevier, Amsterdam, 2007.
33 J. Boita, L. Nicolao, M. C. M. Alves and J. Morais, *Phys. Chem. Chem. Phys.*, 2014, **16**, 17640–17647.
34 J. Wang, L. Xu, T. Wang, R. Li, Y. Zhang, J. Zhang and T. Peng, *Adv. Energy Mater.*, 2021, **11**, 2003575.

